



# STRANGE NONCHAOTIC ATTRACTORS OF CHUA'S CIRCUIT WITH QUASIPERIODIC EXCITATION

ZHIWEN ZHU and ZHONG LIU  
*Department of Electronic Engineering,  
Nanjing University of Science and Technology,  
Nanjing, Jiangsu 210094, P. R. China*

Received January 26, 1996; Revised April 16, 1996

This paper focuses attention on strange nonchaotic attractor of Chua's circuit with two-frequency quasiperiodic excitation. Existence of the attractor is confirmed by calculating several characterizing quantities such as Lyapunov exponents, Poincaré maps, double Poincaré maps and so on. Two basic mechanisms are described for the development of the strange nonchaotic attractor from two-frequency quasiperiodic state (torus solution). One of them is torus-doubling bifurcation followed by a smooth transition from the torus attractor to the strange nonchaotic attractor; and another is that the torus does not undergo period-doubling bifurcation at all; instead, the torus attractor gradually becomes wrinkled, and eventually becomes strange but nonchaotic.

## 1. Introduction

Strange nonchaotic attractors refer to attractors which are geometrically strange (fractal) but nonchaotic (no positive Lyapunov exponents). Since the pioneering work of Grebogi *et al.* [1984], several studies have been carried out to show the existence and characterization of the attractors in quasiperiodically forced nonlinear dynamical systems. These include the studies on forced damped pendula [Bondeson *et al.*, 1985; Romeiras & Ott, 1987], quasiperiodically driven van der Pol oscillator [Kapitaniak *et al.*, 1990; Brindley & Kapitaniak, 1990], quasiperiodically excited Ueda's circuit [Liu & Zhu, 1996], quasiperiodically forced circle map [Ding *et al.*, 1989a], two-frequency parametrically forced Duffing oscillator [Heagy & Ditto, 1991] and other classes of quasiperiodically forced maps [Ding *et al.*, 1989b]. These studies have shown that the strange nonchaotic attractors exist in a wide class of the nonlinear dynamical systems and have

specific characteristics which make them different from the other attractors.

Recently, it was shown that there are two common scenarios leading to the strange nonchaotic behaviors. One scenario is intimately tied to the phenomenon of torus-doubling [Bondeson *et al.*, 1985; Ding *et al.*, 1989a; Heagy & Ditto, 1991] and another is connected to the torus breakdown due to the loss of the smoothness [Kapitaniak *et al.*, 1990; Liu & Zhu, 1996]. The works in [Heagy & Hammel, 1994; Zhu & Liu, 1997] revealed the basic mechanisms for the two scenarios by using the quasiperiodically driven logistic maps.

In this paper, we give another example of the quasiperiodically excited nonlinear dynamical system which exhibits the strange nonchaotic attractors and show that the example can be well utilized to illustrate the two mechanisms for the development of the strange nonchaotic attractors. The system is the two-frequency quasiperiodically excited

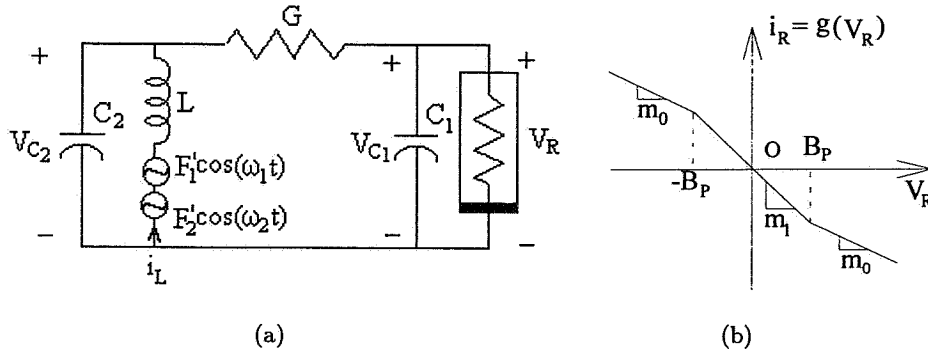


Fig. 1. Circuit realization of the two-frequency quasiperiodically excited Chua's circuit. (a) The circuitry. (b)  $v$ - $i$  characteristic of the nonlinear resistor.

Chua's circuit, as shown in Fig. 1. It should be noted that when both external excitations are zero, the excited circuit becomes the standard Chua's autonomous circuit [Chua *et al.*, 1986; Madan, 1993] and when one of the external excitations is zero, the excited circuit is the periodically excited Chua's circuit [Murali & Lakshmanan, 1991, 1992]. The autonomous Chua's circuit and the periodically excited Chua's circuit have received much research interest and a lot of significant results are well documented in literature [Chua, 1994]. Here we investigate the circuit dynamics when the excitation term contains two incommensurate frequencies. We noticed that the dynamics of two-frequency excited Chua's circuit has been reported [Murali & Lakshmanan, 1993a, 1993b]. The work therein mainly dealt with strange chaotic behavior and its control. In this paper, we will focus our attention on the strange nonchaotic phenomenon which occurs in the quasiperiodically excited circuit.

We have numerically calculated Lyapunov exponents, Poincaré maps and double Poincaré maps of characterizing the circuit behaviors. The results show that the quasiperiodically excited circuit not only possesses the well-known quasiperiodic and strange chaotic solutions, but also has strange nonchaotic solutions. Further simulation analyses reveal that the creation of the strange nonchaotic attractors can be explained by the two developed mechanisms.

This paper is organized as follows: Sec. 2 is background material; Sec. 3 shows the existence of the strange nonchaotic attractors; Sec. 4 describes the development of the attractors and Sec. 5 is the conclusion.

## 2. Background Material

In this section, we introduce the quasiperiodically excited Chua's circuit and several quantities characterizing the various kinds of attractors as a basis for the following study.

The quasiperiodically excited Chua's circuit is shown in Fig. 1. The differential equation describing the circuit is given by

$$\frac{dv_{C_1}}{dt} = \frac{1}{C_1}(G(v_{C_2} - v_{C_1}) - g(v_{C_1})) \quad (1a)$$

$$\frac{dv_{C_2}}{dt} = \frac{1}{C_2}(G(v_{C_1} - v_{C_2}) + i_L) \quad (1b)$$

$$\frac{di_L}{dt} = \frac{1}{L}(-v_{C_2} + F_1' \cos(\omega_1 t) + F_2' \cos(\omega_2 t)) \quad (1c)$$

where  $v_{C_1}$ ,  $v_{C_2}$  and  $i_L$  are the voltage across  $C_1$ , the voltage across  $C_2$  and the current through  $L$ , respectively.  $F_1' \cos(\omega_1 t)$  and  $F_2' \cos(\omega_2 t)$  are two external excitation sources and the frequencies  $\omega_1$ ,  $\omega_2$  are incommensurate. The term  $g(v_{C_1})$  represents the piecewise linear characteristic of Chua's resistor whose functional representation is expressed as

$$i_R = g(V_{C_1}) = m_0 V_{C_1} + 0.5(m_1 - m_0)(|V_{C_1} + B_P| - |V_{C_1} - B_P|) \quad (2)$$

where  $m_0$  is the slope of the first and last segments and  $m_1$  is the slope of the middle segment of the functional curve of the nonlinear resistor as shown in Fig. 1(b).  $B_P$  is the break point voltage.

Depending on the different choices of circuit parameters and excitation parameters ( $F_1'$ ,  $F_2'$ ,  $\omega_1$

and  $\omega_2$ ), the excited circuit exhibits rich dynamics. Now we review several quantities of characterizing the dynamical behaviors.

The first one concerns Lyapunov exponents [Wolf *et al.* 1985]. The Lyapunov exponents provide most direct evidence of divergence or non-divergence of neighboring trajectories. Depending on the sign characteristics of the Lyapunov exponents, we can separate the chaotic attractors from the other attractors. Equation (1) has five Lyapunov exponents; among them there are two trivial exponents which are identically zero by virtue of the two excitation terms. Let the Lyapunov exponents  $\lambda_i$  ( $i = 1, 2, \dots, 5$ ) be ordered by size,  $\lambda_1 \geq \lambda_2 \geq \lambda_3 \geq \lambda_4 \geq \lambda_5$ . Then the possible Lyapunov spectra for the various types of behaviors of Eq. (1) are as follows:

- (1) two-frequency quasiperiodic attractors,  $\lambda_1 = \lambda_2 = 0 > \lambda_3$ ;
- (2) three-frequency quasiperiodic attractors,  $\lambda_1 = \lambda_2 = \lambda_3 = 0 > \lambda_4$ ;
- (3) strange chaotic attractors,  $\lambda_1 > 0$ , and
- (4) strange nonchaotic attractors, with Lyapunov spectrum the same as that of two-frequency quasiperiodic attractors.

We will use the ODE program in [Wolf *et al.* 1985] to perform the calculations of the Lyapunov exponents.

The next quantity is Poincaré map [Guckenheimer & Homels, 1983]. The system (1) has five-dimensional phase space  $(v_{C_1}, v_{C_2}, i_L, \theta_1 = \omega_1 t, \theta_2 = \omega_2 t) \in \mathbf{R}^3 \times S^1 \times S^1$ , where  $S^1 = \mathbf{R}/2\pi$  is the circle of length  $2\pi$ . The Poincaré map is obtained by defining a four-dimensional cross-section to the five-dimensional phase space by fixing the phase of one of the angular variables and allowing the remaining four variables that start on the cross-section to evolve in time under the effect of the flow generated by (1) until they return to the cross-section. If we fix the phase  $\theta_1$ , and define the cross-section as

$$\begin{aligned} \Sigma^{\theta_{10}} &= \{(v_{C_1}, v_{C_2}, i_L, \theta_1, \theta_2) \\ &\in \mathbf{R}^3 \times S^1 \times S^1 | \theta_1 = \theta_{10}\}, \end{aligned} \quad (3)$$

then the Poincaré map  $P^{\theta_{10}}: \Sigma^{\theta_{10}} \rightarrow \Sigma^{\theta_{10}}$  for the flow of Eq. (1) is given by

$$\begin{aligned} P^{\theta_{10}} : (v_{C_1}(0), v_{C_2}(0), i_L(0), \theta_{20}) \\ \rightarrow (v_{C_1}(T), v_{C_2}(T), i_L(T), \theta_{20} + \omega_2 T) \end{aligned} \quad (4)$$

where  $(v_{C_1}(t), v_{C_2}(t), i_L(t), \omega_1 t + \theta_{10}, \omega_2 t + \theta_{20})$  is a solution of Eq. (1) and  $T = 2\pi/\omega_1$  is the period with respect to the frequency  $\omega_1$ . To describe the surface of the Poincaré map, we often plot the projections of the Poincaré map on to planes  $(v_{C_1}, v_{C_2})$ ,  $(v_{C_1}, i_L)$  and  $(v_{C_2}, i_L)$ , respectively. Alternative surfaces can also be obtained by plotting  $v_{C_1}$ ,  $v_{C_2}$  and  $i_L$  against  $\theta_1 \bmod 2\pi$ , respectively. Thus the two-frequency quasiperiodic solution (1-torus solution) corresponds to a closed curve in the  $(v_{C_1}, v_{C_2})$ ,  $(v_{C_1}, i_L)$  and  $(v_{C_2}, i_L)$ , and to a branch in other planes. The strange solution is fractal in all surfaces. However, the three-frequency torus solution is hard to detect by the Poincaré map because its structure is also very complicated [Anishchenko *et al.*, 1994; Parker & Chua, 1989].

Finally we describe the double Poincaré map, which is useful to uncover the fractal properties of the attractor in the two-frequency quasiperiodically forced systems. See [Moon, 1987] for the exposition of the idea. With respect to Eq. (3), we define a double Poincaré section as

$$\begin{aligned} \Sigma^{\theta_{10}, \theta_{20}, \Delta\theta_{20}} &= \{(v_{C_1}, v_{C_2}, i_L, \theta_1, \theta_2) \\ &\in \mathbf{R}^3 \times S^1 \times S^1 | \theta_1 = \theta_{10}, \theta_2 \in [\theta_{20}, \theta_{20} + \Delta\theta_{20}]\} \end{aligned} \quad (5)$$

where  $\Delta\theta_{20}$  is small. Then the double Poincaré map  $\Phi^{\theta_{10}, \theta_{20}, \Delta\theta_{20}}: (v_{C_1}, v_{C_2}, i_L) \rightarrow (v_{C_1}, v_{C_2}, i_L)$  is obtained by sampling solutions of Eq. (1) when the phase of the first excitation term equals  $\theta_{10}$  and the phase of the second excitation term is involved in the interval  $[\theta_{20}, \theta_{20} + \Delta\theta_{20}]$ . Thus the double Poincaré map is approximately considered as a three-dimensional map when  $\Delta\theta_{20}$  is very small. An invariant 1-torus of the Poincaré map corresponds to an invariant small segment of the double Poincaré map, the projection of which on to the  $(v_{C_1}, v_{C_2})$ -plane looks like a single point. With the three-frequency quasiperiodical solution present, one may see a closed curve in the double Poincaré map. The fractal-like structure of strange attractors is also revealed for double Poincaré map.

By using the Poincaré map and the double Poincaré map, we can differentiate the strange nonchaotic attractors from the quasiperiodic attractors.

### 3. Existence of Strange Nonchaotic Attractors

The dynamics associated with (1) depends on seven circuit parameters and four excitation parameters.

In this section, we will choose  $F_2$  as a variable parameter while fixing the other parameters as:<sup>1</sup>

$$\begin{aligned} 1/C_1 = 6, 1/C_2 = 1, 1/L = 7, G = 0.7 \\ m_0 = -0.5, m_1 = -0.8, B_P = 1 \\ F'_1 = 1, \omega_1 = 1, \omega_2 = (\sqrt{5} - 1)/2 \end{aligned}$$

In the simulation studies, we choose  $\theta_{10} = 0$ ,  $\theta_{20} = 0$  and  $\Delta\theta_{20} = 2\pi \times 0.01$  for the calculation of Poincaré maps and double Poincaré maps. For the calculation of Lyapunov exponents, the number of driver periods corresponding to  $\omega_1$  was taken between  $2 \times 10^3$  and  $1 \times 10^6$  depending on the convergence.

The existence of the strange nonchaotic attractors can be best understood by observing the Lyapunov exponents, Poincaré maps and double Poincaré maps. Figure 2 shows the plot of the largest Lyapunov exponent  $\lambda_{\max}$  (except two trivial exponents) against  $F_2$ . Depending on the system behaviors (as discussed below), we have divided the parameter into five regions. For the Regions I and III, the largest Lyapunov exponent is positive, and hence it is easy to detect that the circuit is in strange chaotic state when the parameter  $F_2$  falls in those regions. Figure 3 shows the projections of the Poincaré map and the double Poincaré map on to  $(v_{C_1}, v_{C_2})$ -plane, with the parameter  $F_2$  (equals to 0.4) taken from the Regions I. (In this section and the following discussions, without ambiguity, the Poincaré maps and the double

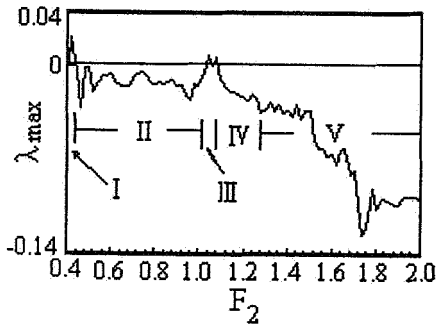


Fig. 2. The largest Lyapunov exponent  $\lambda_{\max}$  of (1) against  $F_2$ .

Poincaré maps refer to their projections on to the appropriate planes.) For Regions II, IV and V, the largest Lyapunov exponent is nonpositive. As we noted in Sec. 2, these regions are possible regions where the strange nonchaotic attractors exist. However, for parameter  $F_2$  in Region V, the Poincaré map and double Poincaré map show simple structures. Figure 4 gives an example with  $F_2 = 2$ . As seen, the Poincaré map is a closed curve and the double Poincaré map looks like a point. Hence, the attractor is a two-frequency quasiperiodic attractor. We have tested other parameters in Region V and the results are the same. This implies that the circuit is quasiperiodic when we select parameter  $F_2$  in Region V. When the parameter  $F_2$  is in the Regions II and IV, the situations are quite different. Figures 5 and 6 give the Poincaré maps and the double Poincaré maps for parameter  $F_2 = 1$  and 1.2, respectively. It is noted that the Poincaré maps and the double Poincaré maps are quite different from these in Fig. 4. They are fractal! In other words, the circuit behaviors are strange. Because of nonpositive Lyapunov exponent, we can say that the circuit works in the strange nonchaotic state. For other parameters  $F_2$  in Regions II and IV, the circuit performs the same dynamical behavior. Based on these observations, we may conclude that the circuit has the strange nonchaotic behaviors and the behaviors are typical in the sense that they exist in substantial parameter ranges. For the current selection of the circuit and excitation parameters, it seems that the strange nonchaotic attractors are much more general than the strange chaotic attractors are. Finally, we point out that there exists three-frequency quasiperiodic behavior at the transition of the strange nonchaotic and chaotic behaviors (corresponding to the largest Lyapunov exponent of zero). However, it is difficult to observe the behavior because it exists on a set of zero Lebesgue measure in the  $F_2$  parameter.

In this section we have studied the effect of the external quasiperiodic excitation on Chua's circuit dynamics. The results have shown that the quasiperiodically excited circuit indeed has the strange nonchaotic behaviors. For the easy presentation, we have only studied the circuit dynamics effected by one of two excitation signals. We also find the existence of the strange nonchaotic attractors for some other parameter settings. We will elaborate this in the next section along with the discussion of the mechanisms for the birth of strange nonchaotic attractors.

<sup>1</sup>For convenience, let  $F_2 = F'_2/L$  in the following.

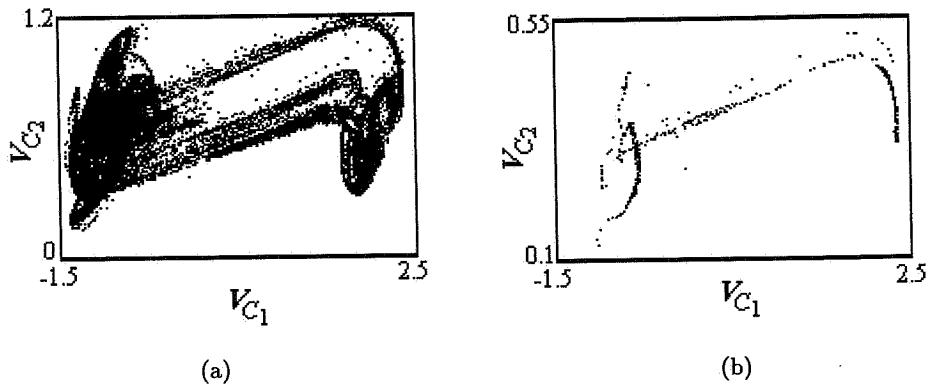


Fig. 3. Poincaré map (a) and double Poincaré map (b) of (1) for  $F_2 = 0.4$ .

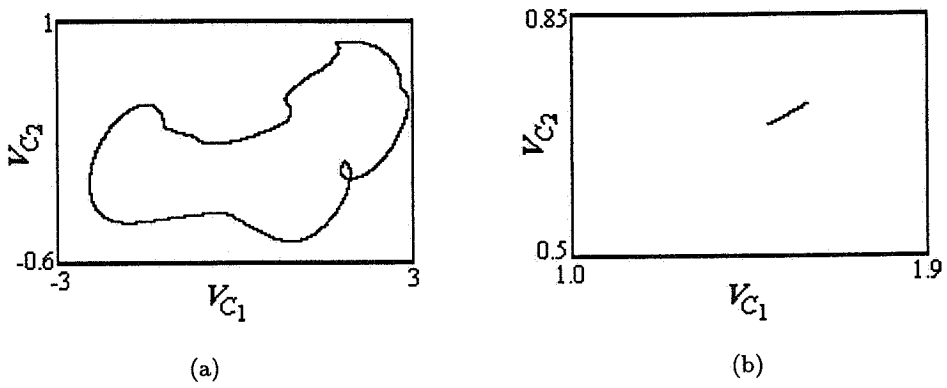


Fig. 4. Poincaré map (a) and double Poincaré map (b) of (1) for  $F_2 = 2$ .

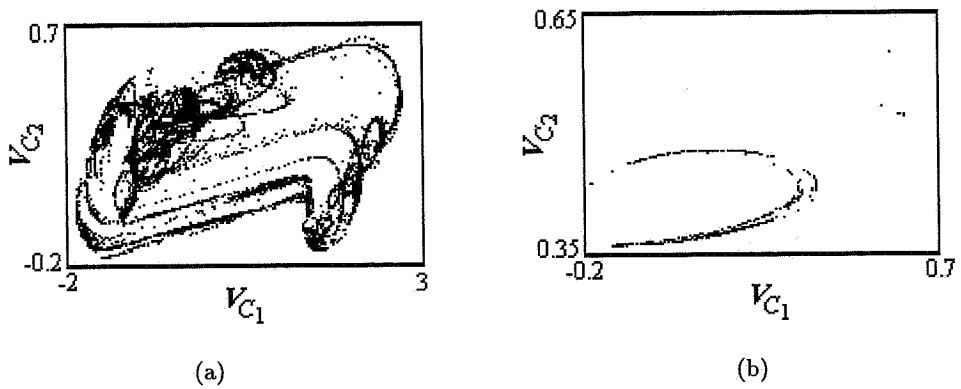


Fig. 5. Poincaré map (a) and double Poincaré map (b) of (1) for  $F_2 = 1$ .

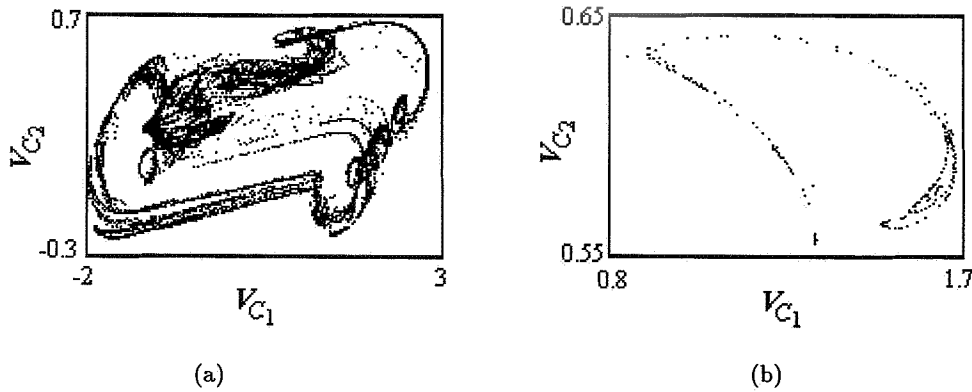


Fig. 6. Poincaré map (a) and double Poincaré map (b) of (1) for  $F_2 = 1.2$ .

#### 4. The Birth of Strange Nonchaotic Attractors

In this section, we describe two scenarios for the birth of the strange nonchaotic attractors from two-frequency quasiperiodic behaviors and discuss the corresponding mechanisms. One scenario is torus-doubling bifurcation followed by a smooth transition from the two-frequency torus attractor to the strange nonchaotic attractor. Another scenario is that the torus does not undergo period-doubling cascade as system parameters vary, instead, torus curve becomes extremely wrinkled, loses its smoothness and finally becomes fractal.

##### 4.1. The first scenario: torus-doubling phenomenon [Heagy & Hammel, 1994]

Let the parameter  $F_2 = 0.01$ ,  $1/C_1$  vary between 6.5 and 7 and the other parameters be as prescribed in the last section. Figure 7 shows the evolution of typical attractors as  $1/C_1$  varies. From this figure, we can depict the creation of the strange nonchaotic behaviors by the torus-doubling phenomenon. When  $1/C_1 = 6.55$ , the excited Chua's circuit has its basic solution: two-frequency torus. This is obvious from the Poincaré map and the double Poincaré map shown in Figs. 7(a) and (b). As  $1/C_1$  increases, for example  $1/C_1 = 6.8$ , the Poincaré map [Fig. 7(c)] becomes two smooth branches and the double Poincaré map [Fig. 7(d)] becomes two points or two segments. Thus the circuit behavior becomes  $2 \times$  torus attractor. As discussed in [Heagy & Hammel, 1994], the  $2 \times$  torus is created by a period-doubling (torus-doubling) bifurcation from the period-1 repeller. As  $1/C_1$  further increases, the

torus attractor does not undergo bifurcation further but becomes wrinkled, as shown in Fig. 7(e) for  $1/C_1 = 6.88$ . But the double Poincaré map shown in Fig. 7(f) indicates that the circuit is still in the quasiperiodic state. (The magnified view of Fig. 7(e) shown in Fig. 7(g) reveals that the attractor is still smooth. In fact, the branches of the  $2 \times$  torus are close to the 1-period repeller [Heagy & Hammel, 1994].) As  $1/C_1$  increases, the two branches become extremely wrinkled and result in a strange attractor. This is reflected in the Poincaré map and the double Poincaré map shown in Figs. 7(h) and 7(i) for  $1/C_1 = 6.89$ . Figure 7(j) is a magnified view of Fig. 7(h). Figure 7(j) indicates the apparent discontinuity in the Poincaré map. However, during this sequence, the largest Lyapunov exponent  $\lambda_{\max}$  remains negative, which is shown in Fig. 8. Therefore, we conclude that the circuit works in the strange nonchaotic state for  $1/C_1 = 6.89$ . As  $1/C_1$  further increase, there is an eventual transition to the strange chaotic attractor, the Poincaré map and double Poincaré map for  $1/C_1 = 7$  are shown in Fig. 7(k) and Fig. 7(l), respectively.

The results in this section show that the circuit behavior is bifurcated into  $2 \times$  torus from its basic torus as  $1/C_1$  increases. After that, the circuit attractor becomes strange nonchaotic as  $1/C_1$  further increases. The evolution of the strange nonchaotic attractors was first suggested by Heagy and Hammel [1994] in the quasiperiodically excited logistic map. Here we find a continuous system which bears a resemblance to that. In the above analysis, we have chosen the circuit parameters which make the circuit become strange nonchaotic after the first-order torus bifurcation. In fact, the circuit parameters can be selected to have high-order bifurcations and after that the circuit becomes strange nonchaotic. We will discuss this in another paper.

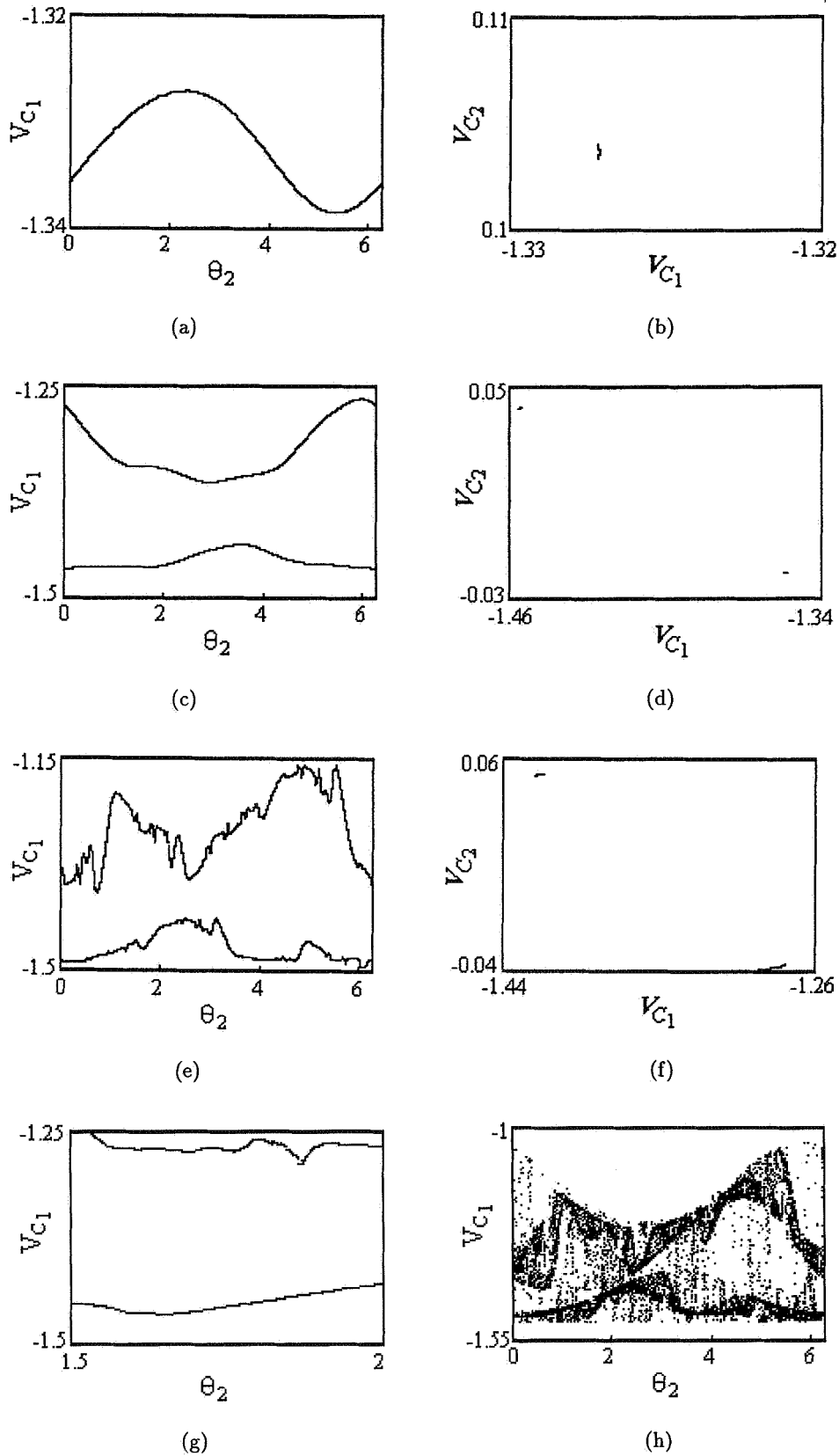


Fig. 7. The evolution of typical attractors from two-frequency quasiperiodic to strange chaotic as  $1/C_1$  increases when  $F_2 = 0.01$ . (a) The Poincaré map for  $1/C_1 = 6.55$ ; (b) the double Poincaré map for  $1/C_1 = 6.55$ ; (c) the Poincaré map for  $1/C_1 = 6.8$ ; (d) the double Poincaré map for  $1/C_1 = 6.8$ ; (e) the Poincaré map for  $1/C_1 = 6.88$ ; (f) the double Poincaré map for  $1/C_1 = 6.88$ ; (g) the local magnified view of (e); (h) the Poincaré map for  $1/C_1 = 6.89$ ; (i) the double Poincaré map for  $1/C_1 = 6.89$ ; (j) the local magnified view of (h); (k) the Poincaré map for  $1/C_1 = 7$ ; (l) the double Poincaré map for  $1/C_1 = 7$ .

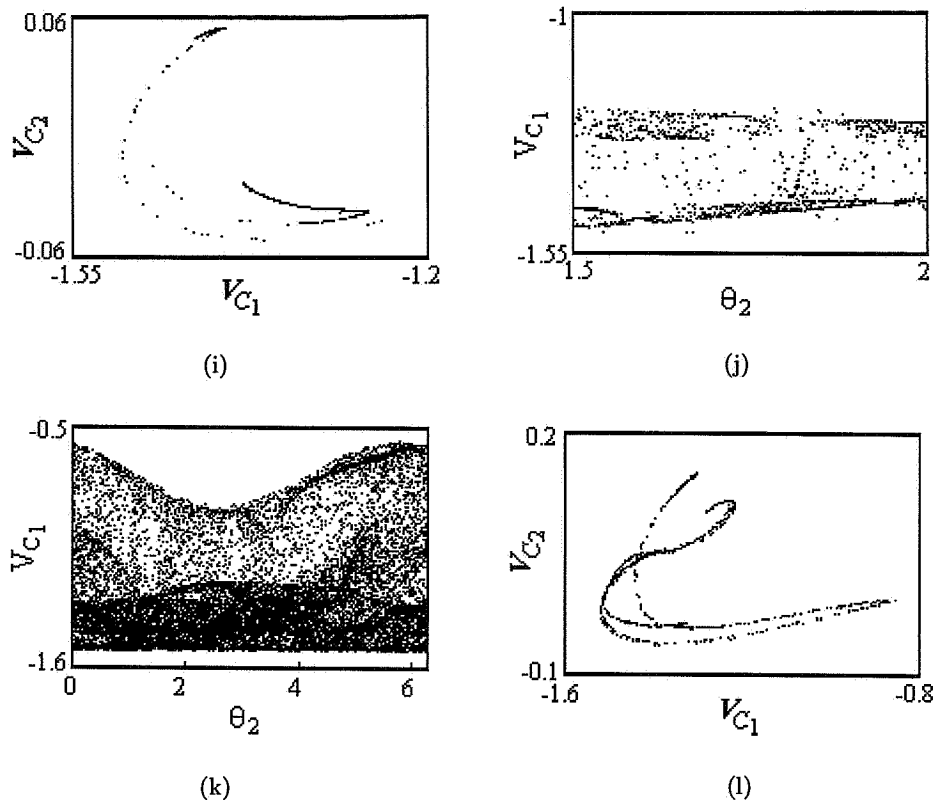


Fig. 7. (Continued)

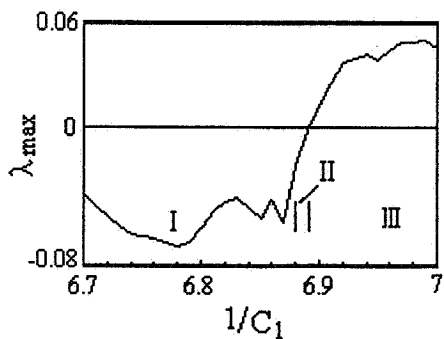


Fig. 8. The largest Lyapunov exponent  $\lambda_{\max}$  against  $1/C_1$  when  $F_2 = 0.01$ . (Region I corresponds to quasiperiodic state; Region II to strange nonchaotic state; and Region III to chaotic state.)

**4.2. The second scenario: torus breakdown due to the loss of smoothness [Zhu & Liu, 1997]**

In this scenario, we fix the parameter  $F_2 = 0.05$  and let  $1/C_1$  vary from 6.8 to 6.87. Attractors for successively larger  $1/C_1$  are shown in Fig. 9. For  $1/C_1 = 6.8$ , the Poincaré map [Fig. 9(a)] of

the attractor has one smooth branch and its double Poincaré map [Fig. 9(b)] is a small segment. This indicates that the circuit is in two-frequency torus state. As  $1/C_1$  increases, the attractor does not undergo torus-doubling bifurcation as in the first scenario; instead, the branch in the Poincaré map becomes irregular as shown in Fig. 9(c) for  $1/C_1 = 6.85$ . But its double Poincaré map shown in Fig. 9(d) is still a small segment, and the magnified view of Fig. 9(c) shown in Fig. 9(e) indicates that the attractor is continuous. In other words, the circuit is still in torus state. As  $1/C_1$  increases further, the attractor becomes extremely wrinkled, and ultimately results in fractal phenomenon. Figures 9(f) and 9(g) show the Poincaré map and double Poincaré map for  $1/C_1 = 6.86$ , respectively. Figure 9(h) is a magnified view of Fig. 9(f). It is seen that the attractor is strange. Figure 10 shows the largest Lyapunov exponent  $\lambda_{\max}$  (except two trivial exponents) of circuit against  $1/C_1$ . Combining Fig. 10 and Figs. 9(f)–9(h), we can say that the circuit is strange nonchaotic for  $1/C_1 = 6.86$ . As  $1/C_1$  increases further, the circuit eventually transmits to chaotic state from nonchaotic state. Figures 9(i) and 9(j) present the Poincaré map and



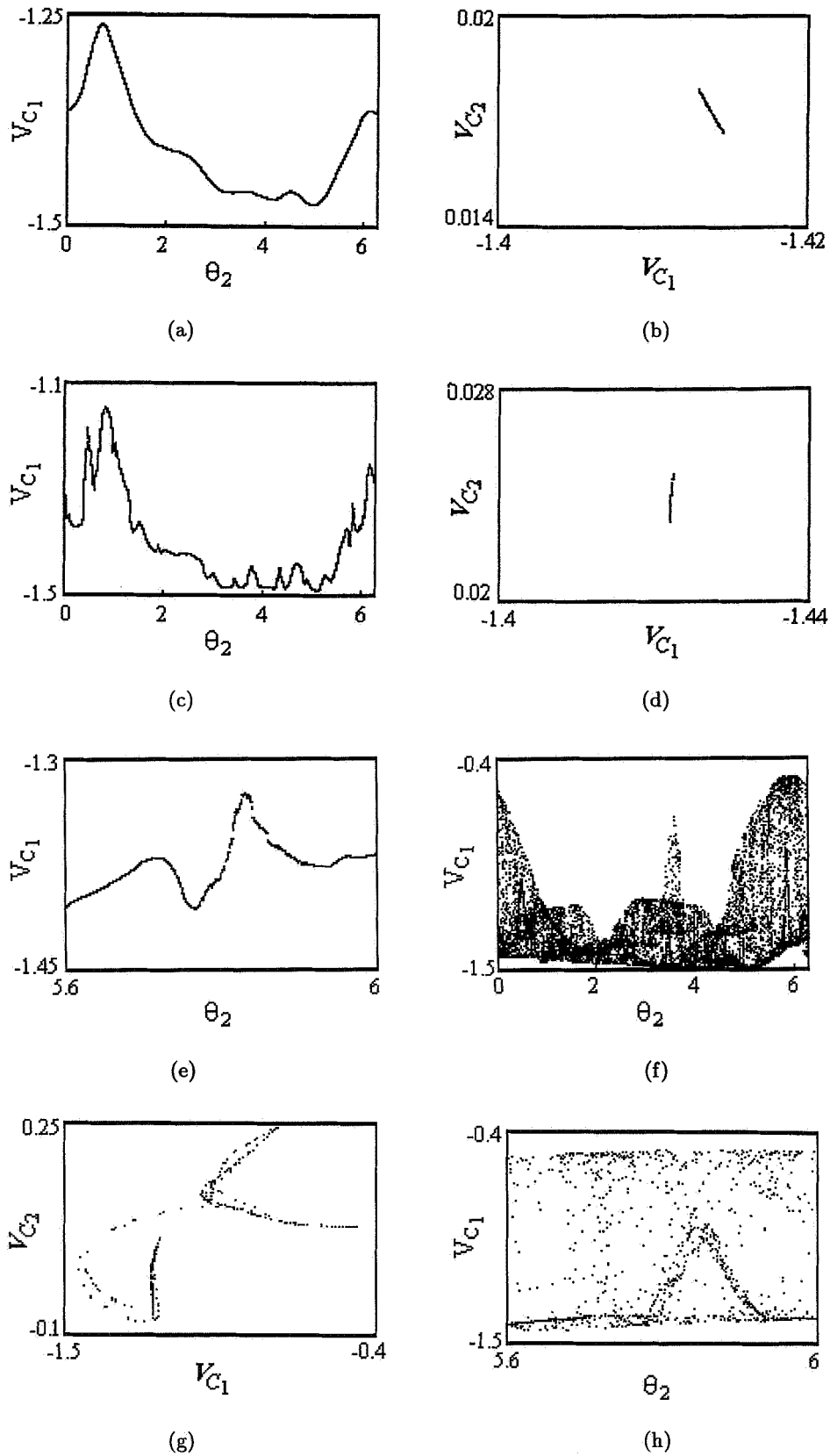


Fig. 9. The evolution of typical attractors from two-frequency quasiperiodic to strange chaotic as  $1/C_1$  increases when  $F_2 = 0.05$ . (a) The Poincaré map for  $1/C_1 = 6.8$ ; (b) the double Poincaré map for  $1/C_1 = 6.8$ ; (c) the Poincaré map for  $1/C_1 = 6.85$ ; (d) the double Poincaré map for  $1/C_1 = 6.85$ ; (e) the local magnified view of (c); (f) the Poincaré map for  $1/C_1 = 6.86$ ; (g) the double Poincaré map for  $1/C_1 = 6.86$ ; (h) the local magnified view of (f); (i) the Poincaré map for  $1/C_1 = 6.87$ ; (j) the double Poincaré map for  $1/C_1 = 6.87$ .

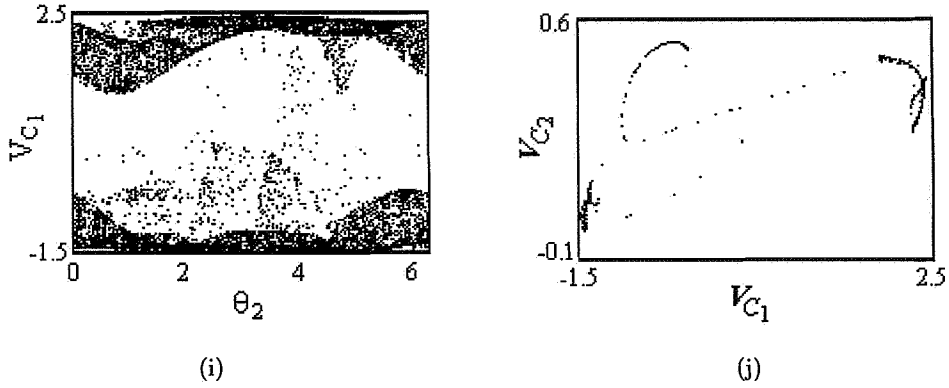


Fig. 9. (Continued)

double Poincaré map of chaotic attractor for  $1/C_1 = 6.87$ .

The development of the strange nonchaotic attractors is tied to torus breakdown phenomenon [Anishchenko *et al.*, 1993; Zhu & Liu, 1997]:

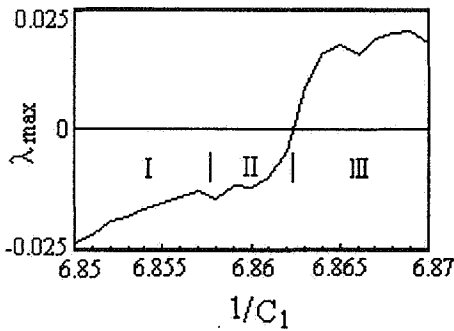


Fig. 10. The largest Lyapunov exponent  $\lambda_{max}$  against  $1/C_1$  when  $F_2 = 0.05$ . (Region I corresponds to quasiperiodic state; Region II to strange nonchaotic state; and Region III to chaotic state.)

the torus first becomes wrinkled, then loses its smoothness and finally becomes fractal. However the largest Lyapunov exponent remains negative during the process. The torus breakdown due to the loss of smoothness formulates a soft transition to strange nonchaotic attractor from quasiperiodic attractor.

The mechanism of the torus breakdown due to the loss of smoothness is also applicable to the strange nonchaotic attractors in Sec. 3. Figure 11 shows the evolution of the attractors as  $F_2$  varies. The evolution is the same as discussed in the above. We will not elaborate it here.

### 5. Conclusion

Chua's circuit is one of the simplest circuits which exhibit the strange behaviors. Because of its simplicity, it has become a fundamental block for studying various nonlinear dynamical phenomena [Murali & Lakshmanan, 1992; Chua, 1994]. In this paper, we have briefly investigated the effect of the

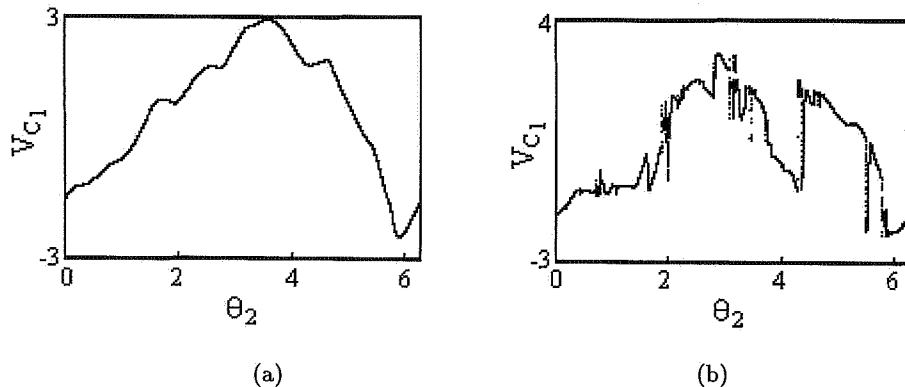


Fig. 11. The sequence of attractors as  $F_2$  varies when  $1/C_1 = 6$ . (a) The Poincaré map for  $F_2 = 2$ ; (b) the Poincaré map for  $F_2 = 1.6$ ; (c) the local magnified view of Poincaré map for  $F_2 = 1.6$ ; (d) the Poincaré map for  $F_2 = 1$ ; (e) the local magnified view of Poincaré map for  $F_2 = 1$ ; (f) the Poincaré map for  $F_2 = 0.4$ .

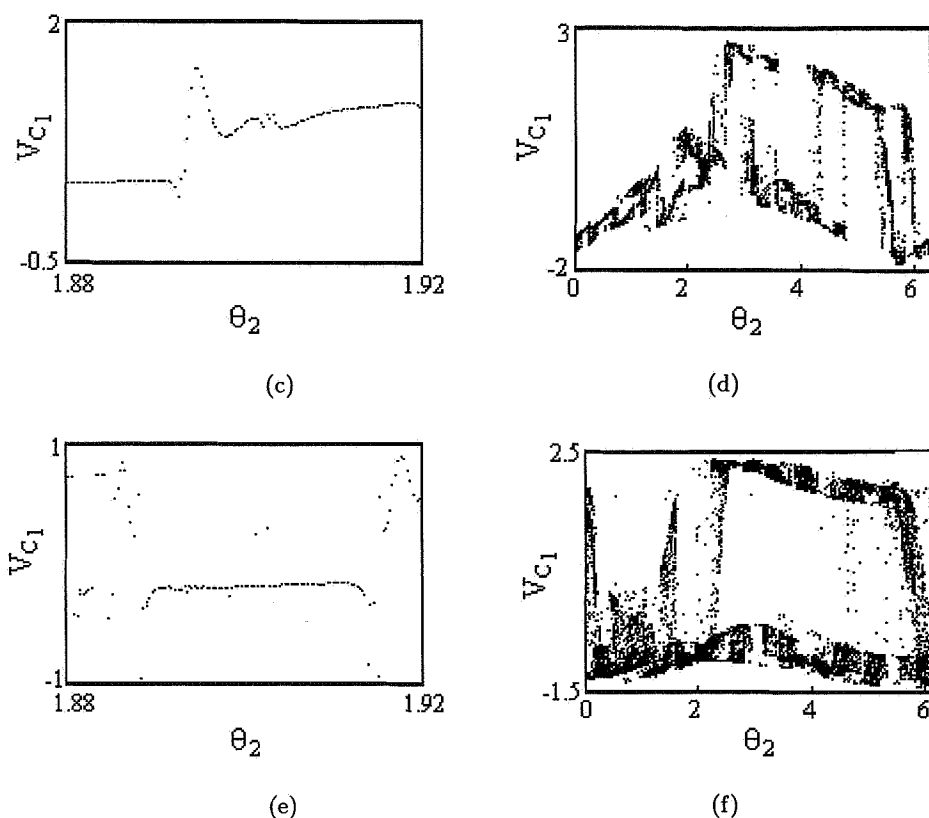


Fig. 11. (Continued)

quasiperiodic excitation on the dynamics of Chua's circuit. Our researches have shown that the excited Chua's circuit not only possesses the strange nonchaotic behaviors but can also be used to study the development of the attractors. Thus this study reveals that this circuit can be effectively utilized to study the strange nonchaotic phenomena. Chua's circuit is a piecewise linear circuit. Analytical methods are available for the investigations of nonlinear dynamics in the circuit. It is expected that the analytical methods can also be developed for the study of the strange nonchaotic behaviors in the quasiperiodically excited Chua's circuit.

### Acknowledgment

The authors would like to thank referees for their valuable comments and suggestions, which improved the quality of this paper very much. This work was supported in part by the Return-Scholar Foundation and the Excellent Young Teacher Foundation of the National Education Commission and by the Jiangsu Natural Science Foundation.

### References

- Anishchenko, V. S., Safonova, M. A. & Chua, L. O. [1993] "Confirmation of the Afraimovich-Shilnikov torus-breakdown theorem via a torus breakdown," *IEEE Tran. Circ. Syst. I: Fundamental Theory Applications* **40**, 792–800.
- Anishchenko, V. S., Safonova, M. A., Feudel, U. & Kurths, J. [1994] "Bifurcations and transition to chaos through three-dimensional tori," *Int. J. Bifurcation and Chaos* **4**(3), 595–607.
- Bondeson, A., Ott, E. & Antonsen, T. M. [1985] "Quasiperiodically forced damped pendula and Schrodinger equations with quasiperiodic potentials: implications of their equivalence," *Phys. Rev. Lett.* **55**, 2103–2106.
- Brindley, J. & T. Kapitaniak, T. [1991] "Existence and characterization of strange nonchaotic attractors in nonlinear systems," *Chaos, Solitons and Fractals* **1**, 323–337.
- Chua, L. O., Komuro, M. & Matsumoto, T [1986] "The double-scroll family," *IEEE Trans. Circ. Syst.* **33**, 1072–1118.
- Chua, L. O. [1994] "Chua's circuit 10 years later," *Int. J. Cir. Theor. Appl.* **22**, 279–305.
- Ding, M., Grebogi, C. & Ott, E. [1989a] "Evolution of attractors in quasiperiodically forced systems: From

- quasiperiodic to strange nonchaotic to chaotic," *Phys. Rev.* **A39**, 2593–2598.
- Ding, M., Grebogi, C. & Ott, E. [1989b] "Dimensions of strange nonchaotic attractors," *Phys. Lett.* **A137**, 167–172.
- Grebogi, C., Ott, E., Pelikan, S. & Yorke, J. A. [1984] "Strange attractors that are not chaotic," *Physica* **D13**, 261–268.
- Guckenheimer, J. & Holmes, P. J. [1983] *Nonlinear Oscillations, Dynamical Systems, and Bifurcations of Vector Fields* (Springer-Verlag, New York).
- Heagy, J. F. & Ditto, W. L. [1991] "Dynamics of a two-frequency parametrically driven Duffing oscillator," *J. Nonlin. Sci.* **1**, 423–455.
- Heagy, J. F. & Hammel, S. M. [1994] "The birth of strange nonchaotic attractors," *Physica* **D70**, 140–153.
- Kapitaniak, T., Ponce, E. & Wojewada, J. [1990] "Route to chaos via strange nonchaotic attractors," *J. Phys. A: Math. Gen.* **23**, L383–L387.
- Liu, Z. & Zhu, Z. W. [1996] "Strange nonchaotic attractors from quasiperiodically forced Ueda's circuit," *Int. J. Bifurcation and Chaos* **6**(7), 1383–1388.
- Madan, R. N. [1993] *Chua's Circuit: A Paradigm for Chaos* (World Scientific, Singapore).
- Moon, F. C. [1987] *Chaotic Vibration: An Introduction for Applied Scientist and Engineers* (John Wiley & Sons, New York).
- Murali, K. & Lakshmanan, M. [1991] "Bifurcation and chaos of the sinusoidally driven Chua's circuit," *Int. J. Bifurcation and Chaos* **1**, 369–384.
- Murali, K. & Lakshmanan, M. [1992] "Effect of sinusoidal excitation on the Chua's circuit," *IEEE Trans. Circ. Syst. I: Fundamental Theory Applications* **39**, 264–270.
- Murali, K. & Lakshmanan, M. [1993a] "Chaotic dynamics of the driven Chua's circuit," *IEEE Trans. Circ. Syst. I: Fundamental Theory Applications* **40**, 836–840.
- Murali, K. & Lakshmanan, M. [1993b] "Controlling of chaos in the driven Chua's circuit," *J. Circ. Syst. Comput.* **3**, 591–601.
- Parker, T. & Chua, L. O. [1990] *Practical Numerical Algorithms for Chaotic Systems* (Springer-Verlag, New York).
- Romeiras, F. J. & Ott, E. [1987] "Strange nonchaotic attractors of the damped pendulum with quasiperiodic forcing," *Phys. Rev.* **A35**, 4404–4413.
- Wolf, A., Swift, J. B., Swinney, H. L. & Vasano, J. A. [1985] "Determining Lyapunov exponents from a times series," *Physica* **D16**, 285–317.
- Zhu, Z. W. & Liu, Z. [1997] "Strange nonchaotic attractor via torus breakdown," *Int. J. Bifurcation and Chaos*.